Research Paper

Journal of Chemical Research

Journal of Chemical Research
1–8

DOI: 10.1177/1747519820910384
journals.sagepub.com/home/chl
SAGE

Design, synthesis, and biological evaluation of quinazoline derivatives containing piperazine moieties as antitumor agents

Wen Li[1], Shu-Yi Chen[1], Wei-Nan Hu[1], Mei Zhu[1], Jia-Min Liu[1], Yi-Hong Fu[1], Zhen-Chao Wang[1,2] and Gui-Ping OuYang[1,2,3]

Abstract

A series of novel quinazoline derivatives containing piperazine analogs are synthesized via substitution reactions with 6,7-disubstituted 4-chloroquinazoline and benzyl piperazine (amido piperazine). Potent antiproliferative activities are observed against A549, HepG2, K562, and PC-3 with *N*-(3-chlorophenyl)-2-(4-(7-methoxy-6-(3-morpholino-propoxy) quinazoline-4-yl)piperazine-1-yl)acetamidename **C9** showing excellent activity. This active derivative was screened for cell migration ability, proliferation effects, and apoptosis against A549 and PC-3 cells, with the result showing biological activity almost equal to that of the control gefitinib.

Keywords

quinazoline derivatives, cytotoxicity, migratory capacity, colonization activity, apoptosis

Date received: 1 December 2019; accepted: 10 February 2020

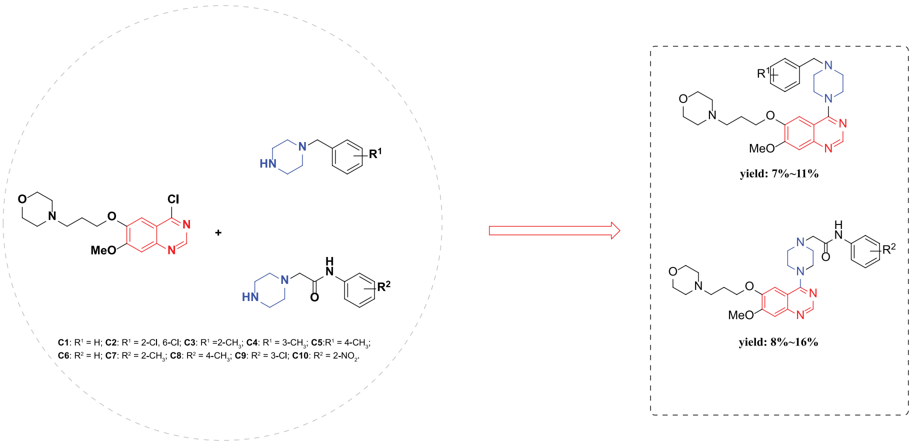

Introduction

It has been reported that the quinazoline unit is of great value as a chemical skeleton with diverse pharmaceutical and physiological utility, including antimicrobial,[1] antihyperlipidemic,[2] anticonvulsant,[3] antihypertensive,[4] and anti-inflammatory[5] activities. Therefore, many quinazolines have contributed to the quest for an ultimate antitumor chemotherapeutic agent. Moreover, several small molecules such as gefitinib (Figure 1), erlotinib, and lapatinib, which containing quinazoline analogs, were designed to inhibit epidermal growth factor receptor (EGFR) kinase activity. Among them, gefitinib—an oral small molecule agent that inhibits EGFR tyrosine phosphorylation, was approved by the US Food and Drug Administration (FDA) for locally advanced or metastatic non-small cell lung cancer therapy—is involved in cellular signal-transduction pathways that regulate essential

[1]College of Pharmacy, Guizhou University, Guiyang, P.R. China
[2]State Key Laboratory of Functions and Applications of Medicinal Plants, Guizhou Medical University, Guiyang, P.R. China
[3]Drug Synthetic Engineering Laboratory of Guizhou Province, Guiyang, P.R. China

Corresponding author:
Zhen-Chao Wang, College of Pharmacy, Guizhou University, Guiyang 550025, P.R. China.
Email: wzc.4884@163.com

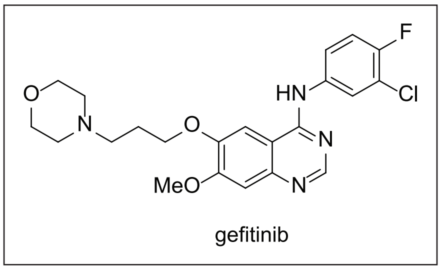

Figure 1. The structure of gefitinib.

functions such as proliferation, differentiation, and apoptosis.[6–14] However, its efficient use is seriously hampered by EGFR mutation. Even though tumors were sensitive to gefitinib, tumor regrowth occurs after several months and all of the mechanisms of the resistance have not been clarified. Thus, it is necessary to exploit novel antitumor drugs with high efficiency and low toxicity due to the various side effects of gefitinib.[15]

Over past decades, a large number of piperazine heterocyclic derivatives have attracted significant attention as chemotherapeutic drugs. Numerous studies have illustrated that the introduction of piperazine moieties can influence the physicochemical properties and enhance the bioactivity of compounds. It is known that piperazine is versatile and privileged in drug discovery,[16–20] for example, in ciprofloxacin for the treatment of bacterial infections, trifluoperazine for psychosis, cetirizine for the treatment of allergies, and tanitinib for the treatment of acute myeloid leukemia. A series of 4-amino-2*H*-benzo(h)chromen-2-one analogs containing the piperazine moiety were reported by Chen in 2019, and bioassays showed that these compounds exhibited potent antagonistic potency against androgen receptors (AR; inhibition $>50\%$), and exhibited potent AR binding affinities as well as displaying higher activities than finasteride toward LNCaP cells (AR-rich) versus PC-3 cells (AR-deficient).[21]

Based on the active substructure combination theory, the piperazine ring was utilized in this research. Thus, two series of novel 4-piperazine quinazoline derivatives were designed and synthesized. The preliminary antitumor activity of these new compounds was also evaluated in vitro. In addition, the primary apoptotic effect mechanism induced by a representative compound **C9** was also investigated by flow cytometry.

Results and discussion

Synthesis

The synthetic route for the preparation of the novel quinazoline derivatives containing a piperazine moiety is summarized in Scheme 1. The key intermediate **7** was synthesized in six steps (a to f). 3-Hydroxy-4-methoxybenzaldehyde (**1**) was chosen as the starting material and was reacted with 1-bromo-3-chloropropane followed by reaction with $NH_2OH{\cdot}HCl$, AcOH, and AcONa to form 3-(3-chloropropoxy)-4-methoxybenzonitrile (**3**). This was subjected to nitration using nitric acid and the product **4** reacted with morpholine under potassium iodide (KI) catalysis to give intermediate **5**. This was converted to the quinazoline **7** by reduction with hydrazine hydrate followed by ring closure using formic acid and chlorination.[22] As shown in route 1, intermediate **7** was reacted with a series of monosubstituted piperazines **8** to give the target compounds **C1**–**C5**. In addition, intermediate **7** was reacted with a series of amide-containing monosubstituted piperazines **9** to give the target compounds **C6**–**C10** (route 2). All the target compounds were characterized, and the structures were confirmed by ^{1}H NMR, ^{13}C NMR, and mass spectrometry. Taking compound **C9** as a representative example, two singlets appeared at 8.41 and 3.91 ppm in CD_3OD attributed to the quinazoline –N=C**H** and –OC**H**$_3$, respectively. In the ^{13}C NMR spectrum, a signal due to C=O was observed at 169.5 ppm.

Biological activity

The antitumor activities of the synthesized compounds against four cell lines were evaluated using gefitinib as the control. The IC_{50} values indicated that the compounds exerted antitumor effects, with varying degrees of antitumor activity against the four cell lines. As shown in Table 1, the IC_{50} values ranged from 35.56 ± 9.39 to $8.24 \pm 1.40\,\mu M$ against A549, from 14.57 ± 5.52 to $5.62 \pm 3.23\,\mu M$ against PC-3, from 56.42 ± 0.14 to $8.63 \pm 0.86\,\mu M$ against HepG2, and from 159.3 ± 14.28 to $15.02 \pm 0.88\,\mu M$ against K562, being typically better than gefitinib (IC_{50} values were $5.475 \pm 1.06\,\mu M$ against A549, $5.99 \pm 1.47\,\mu M$ against PC-3, $31.48 \pm 10.23\,\mu M$ against HepG2, and $13.67 \pm 1.44\,\mu M$ against K562). The cytotoxicities of the target compounds against the normal cell line NRK-52E in vitro are shown in the Supporting Information Figure S1). The result showed that the survival rate of the cells at low concentration was close to 100%, and the cytotoxicity of compound **C9** was the weakest among these compounds.

To further investigate the cell migration ability of compound **C9** with the A549 and PC-3 cell lines, wound healing assays were examined with gefitinib and **C9** at concentrations of 5 μM for 24 h, respectively. Representative micrographs showed that compound **C9** efficiently inhibited A549 and PC-3 migration in comparison with dimethyl sulfoxide (DMSO) in a time-dependent manner. Furthermore, the migration ratios of A549 ranged from 13.39% to 53.18% and from 12.40% to 51.54%, and the migration ratio of PC-3 from 5.50% to 16.74% and from 3.03% to 12.60% after being cultured with gefitinib and **C9**, respectively (Figure S2).

To evaluate the cell proliferation effects of **C9**, we performed colony formation on the A549 and PC-3 cell lines. The results showed that the colonies presented significant corresponding downregulated trends on A549 and PC-3 cells when stimulated by a range of **C9** doses (1.25, 2.5, 5, 10, and 20 μM). It was obvious that there was very little colony at 20 μM, and the effect of **C9** was in a dose-dependent manner. As Figure S3 shows, the clonogenic ratio of A549 was from 3.87% to 14.53% and that of PC-3 was from 3.60% to 46.13% after being cultured with **C9** at different concentrations (Figure S3).

In order to investigate the induction of apoptosis in A549 and PC-3 cells, the Hoechst staining assay was conducted in

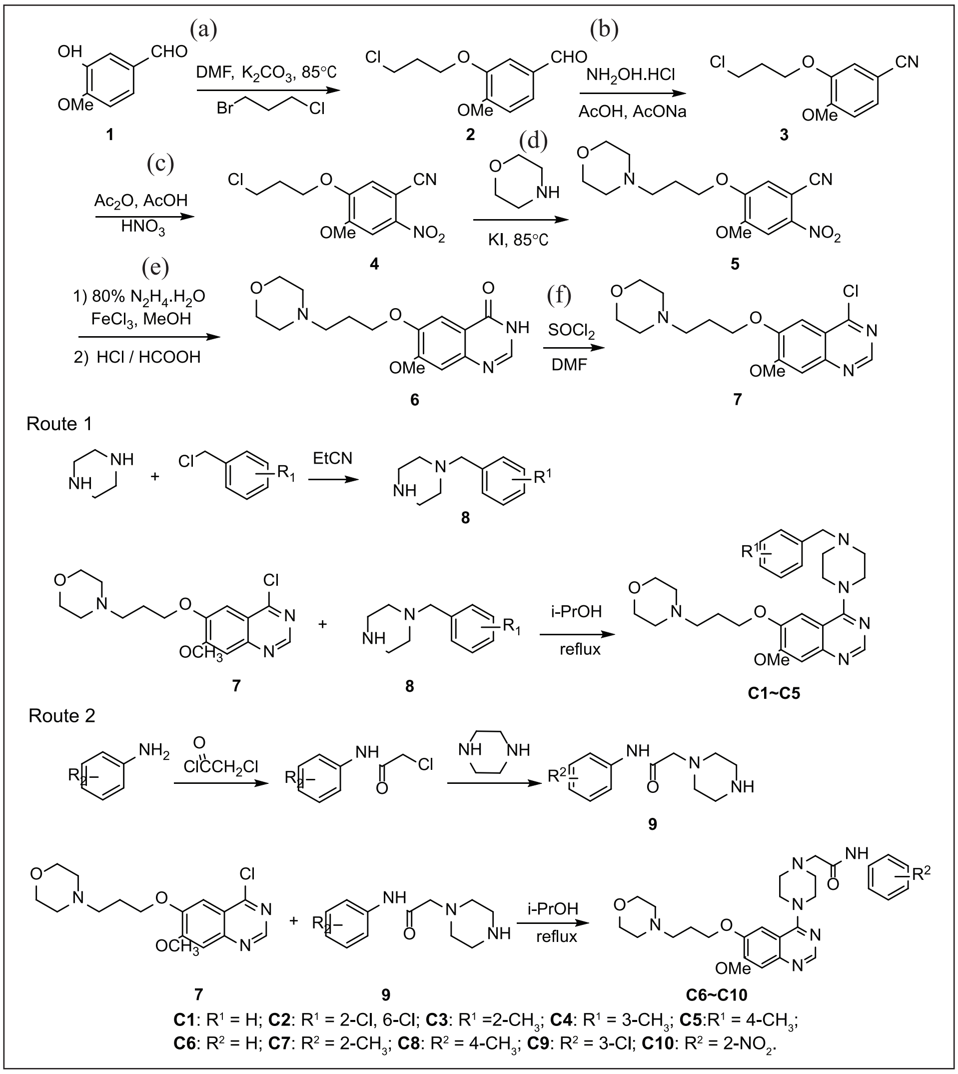

Scheme 1. Synthetic routes to the target compounds **C1–C5** and **C6–C10**.

Table 1. The IC_{50} values of compounds **C1** to **C10** against four cancer cell lines.

IC_{50} (μM)[a]				
Compound	A549	PC-3	HepG2	K562
Gefitinib[b]	5.475 ± 1.06	5.99 ± 1.47	31.48 ± 10.23	13.67 ± 1.44
C1	13.37 ± 6.40	8.19 ± 1.53	24.69 ± 2.73	70.69 ± 10.24
C2	24.85 ± 4.06	14.57 ± 5.52	32.23 ± 3.20	60.94 ± 13.41
C3	13.53 ± 2.35	8.51 ± 3.20	43.45 ± 3.85	15.02 ± 0.88
C4	15.34 ± 7.35	6.44 ± 2.31	29.07 ± 5.65	62.96 ± 13.17
C5	13.94 ± 6.38	5.62 ± 3.23	22.29 ± 2.81	45.52 ± 2.55
C6	8.99 ± 6.29	15.26 ± 5.12	51.29 ± 13.08	17.63 ± 8.20
C7	12.96 ± 1.80	13.72 ± 4.32	31.05 ± 5.53	159.3 ± 14.28
C8	22.51 ± 1.24	13.42 ± 4.87	8.63 ± 0.86	50.00 ± 5.13
C9	8.24 ± 1.40	7.66 ± 1.27	38.62 ± 2.41	21.96 ± 3.51
C10	35.56 ± 9.39	10.42 ± 1.97	40.64 ± 13.18	62.56 ± 5.36

[a]The average of three trials.
[b]Commercial gefitinib was used as a positive control.

nuclear morphology by fluorescent microscopy. As shown in Figure S4, it was easy to observe the distinct pattern of morphological changes, including cell shrinkage, fragmentation of the nucleus, and chromatin condensation after culturing with gefitinib and **C9** at different concentrations (1.25, 2.5, 5, 10, and 20 μM) in A549 and PC-3 cell lines for 24 h (Figure S4).

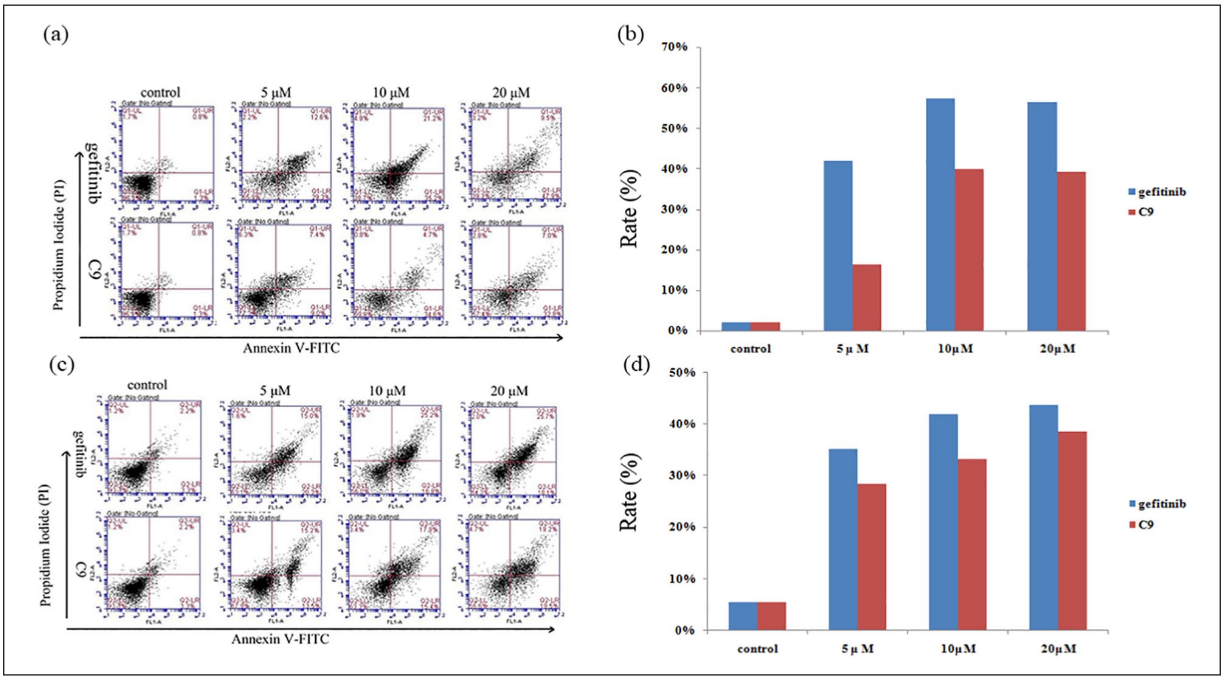

Figure 2. **C9** and gefitinib increase the apoptosis of A549 and PC-3 cells. (a, b) Annexin/PI statin of A549 and (c, d) Annexin/PI statin of PC-3.

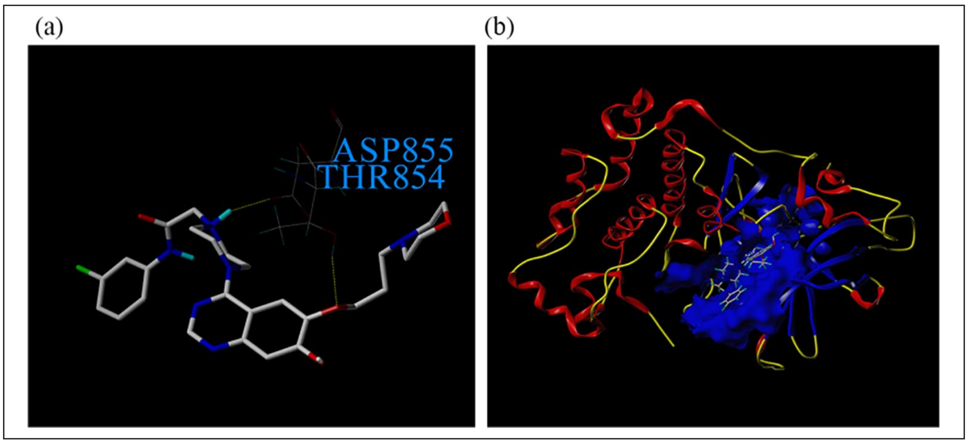

Figure 3. (a) Compound **C9** (colored by atom—carbon: gray, nitrogen: dark blue, oxygen: red, chlorine: green, and hydrogen: blue) is bound into EGFR. The dotted lines show the hydrogen bonds. (b) The surface model structure of binding of compound **C9** with the EGFR complex is shown.

Flow cytometry

Apoptosis assays can provide preliminary information on the mechanism of growth inhibition of tumor cells. Therefore, the apoptotic effects of **C9** against the A549 and PC-3 cell lines were investigated. The results are given in Figure 2. After treatment of A549 and PC-3 cell lines for 24 h with gefitinib and **C9** at different concentrations (5, 10, and 20 µM), the apoptosis ratio of A549 (including the early and late apoptosis rates) was from 41.9% to 57.4% with gefitinib and from 16.4% to 39.8% with **C9**. Furthermore, the apoptosis ratios of PC-3 was from 35.3% to 43.8% with gefitinib and from 28.7% to 38.7% with **C9**, being remarkably influenced by gefitinib and **C9** in a dose-dependent manner.

Binding mode analysis

In order to further evaluate these promising compounds and to guide structure–activity relationship (SAR) studies, the interaction effect between compound **C9** and the EGFR crystal structure (3W2S.pdb) was investigated. Compound **C9** was inserted into the active site of EGFR kinase for molecular docking. All docking runs were applied in Surflex-Dock using Sybyl-X 2.0. The binding mode of compound **C9** and EGFR kinase is depicted in Figure 3. As shown in Figure 3(a), compound **C9** was potently bound to the active site of EGFR kinase by hydrophobic interactions, and the binding mode was stabilized by two hydrogen bonds. The enzyme surface model is shown in Figure 3(b), which revealed that the target molecule **C9** was well embedded in the active pocket of EGFR kinase. This molecular docking result, along with the biological assay data, suggested that compound **C9** was a potential inhibitor of EGFR kinase.

Conclusion

In conclusion, a series of quinazoline derivatives containing a piperazine moiety have been designed and synthesized. Furthermore, the biological activities of these compounds were evaluated according to the Thiazolyl Blue Tetrazolium Bromide (MTT) method, wound healing assay, clonogenic survival assay, Hoechst staining, and flow cytometry. Compound **C9** with excellent activity may represent a promising lead candidate for EGFR-inhibiting therapeutics.

Experimental

Materials and methods

All reagents were purchased from commercial sources as analytical grade and were used without further purification. All reactions were monitored by thin-layer chromatography (TLC). ^{1}H NMR and ^{13}C NMR spectra were performed on a Bruker Ascend 400 NMR (Bruker, Germany) and JEOL-ECX 500 NMR spectrometers (JEOL, Japan) using methanol (CD_3OD) as the solvent and tetramethylsilane as the internal standard. Chemical shifts are expressed in ppm (parts per million) and coupling constants are given in Hz (Hertz). Mass spectra (MS) were recorded on an Agilent 1100 MSD-Trap-VL series with an electron spray ionization (ESI) source. High-resolution mass spectra (HRMS) were recorded on Thermo Scientific Q Exactive series with an ESI source.

The synthesis of intermediate 7. To a solution of **1** in N, N-dimethylformamide (DMF) (40 mL), K_2CO_3 (15.20 g, 0.11 mol) and 1-bromo-3-chloropropane (18.89 g, 0.12 mol) were added. The mixture was stirred and refluxed at 85 °C for 4 h. After completion of the reaction, as monitored by TLC, the solution was added to cold water and the mixture filtered and concentrated under reduced pressure to give the ether **2** (yield 80%). Ether **2** (15.50 g, 0.068 mol), $NH_2OH{\cdot}HCl$ (10 g, 0.136 mol), and AcONa (11.12 g, 0.136 mol) were dissolved in AcOH (40 mL), and the solution was heated at 105 °C for 8 h. After completion of the reaction, as monitored by TLC, the solution was added to saturate sodium chloride (200 mL), and the mixture filtered and concentrated to give the nitrile **3** (yield 90%). Intermediate **3** (17.26 g, 0.076 mol) was added to a mixture of AcOH (50 mL) and Ac_2O (50 mL) keeping the temperature between 0 and 5 °C, and then HNO_3 (40 mL) was added dropwise to the solution. The mixture was stirred and refluxed at room temperature (RT) for 72 h, and then the solution was added to cold water. Ammonia was added to adjust the pH to 7, and then the mixture was filtered and dried to obtain the nitro compound **4** (yield 68%). To a solution of **4** (14.16 g, 0.063 mol) in DMF (40 mL), KI (0.57 g, 0.0035 mol) and morpholine (10.90 g, 0.126 mol) were added. The mixture was stirred and refluxed at 70 °C for 10 h. After the reaction was finished, the mixture was added to cold water, and the solid precipitate was filtered and concentrated to give compound **5** (yield 56%). This intermediate **5** (12.11 g, 0.038 mol) and $FeCl_3$ (0.38 g, 0.002 mol) were dissolved in a mixture of methanol and water (3:1, 120 mL) followed by 80% $N_2H_4{\cdot}H_2O$ (10 mL), and the mixture was heated under reflux (3 h) and then concentrated at 40 °C. Water (37.5 mL), HCl (36%–38%, 45 mL), and HCOOH (>88%, 60 mL) were added to the filtrate until the temperature of reaction mixture reached RT. The mixture was then refluxed at 130 °C for 3.5 h. After completion of the reaction, as evidenced by TLC, the water (75 mL) was added to the mixture until the temperature of the reaction mixture reached RT, after which NaOH was added to adjust the pH to 7. A yellow and white solid was obtained by extracting with $CHCl_3$ (3 mL × 200 mL) and drying the organic layer with anhydrous $MgSO_4$. Ethyl acetate (20 mL) was added into the solid and the solution heated to boiling. The residue was filtered and dried to obtain white solid (**6**) (yield 58%) which could be further converted into key intermediate **7** by reduction with thionyl chloride ($SOCl_2$) in DMF (1.0 g, yield 94%) at 84 °C.

General procedure for the preparation of **C1–C5**. Taking compound **C1** as a representative example, 4-(3-((4-chloro-7-methoxyquinazolin-6-yl)oxy)propyl) morpholine (**7**) (0.50 g, 1.48 mmol), 1-benzylpiperazine (0.31 g, 1.78 mmol), and i-PrOH (15 mL) were added in turn to a flask and refluxed for 4 h. After completion of the reaction, as indicated by TLC, the solvent was evaporated to give a yellowish-brown oily substance. This substance was dissolved in methanol and isolated by column chromatography ($CHCl_3$: MeOH = 15:1). Pure compound was evaporated to give the yellow oily substance (0.08 g, 0.17 mmol).

General procedure for the preparation of **C6–C10**. Taking compound **C6** as a representative example, 4-(3-((4-chloro-7-methoxyquinazolin-6-yl)oxy)propyl) morpholine (0.50 g, 1.48 mmol), *N*-phenyl-2-piperazinyl-acetamide (0.39 g, 1.78 mmol), and i-PrOH (15 mL) were added to a flask and refluxed for 4 h. After completion of the reaction, as indicated by TLC, the solvent was evaporated to give a yellowish-brown oily substance. This substance was dissolved in methanol and isolated by column chromatography ($CHCl_3$: MeOH = 15:1). The pure compound was evaporated to give the brownish black oil substance (0.10 g, 0.19 mmol).

*4-(4-Benzylpiperazin-1-yl)-7-methoxy-6-[3-(4-morpholinyl)propoxy]quinazoline (**C1**).* Yield 11%, 0.08 g; yellow oily substance; ^{1}H NMR (CD_3OD, 500 MHz): δ 8.44 (s, 1H), 7.23–7.35 (m, 5H), 7.12 (s, 2H), 4.12 (t, J = 6.0 Hz, 2H), 3.94 (s, 3H), 3.68–3.70 (m, 8H), 3.58 (s, 2H), 2.49–2.63 (br, m, 10H), 2.03–2.06 (br, m, 2H); ^{13}C NMR (CD_3OD, 125 MHz): δ 163.6, 155.5, 152.0, 148.2, 137.1, 129.3, 128.1, 127.2, 110.6, 105.8, 104.5, 66.9, 66.3, 62.6, 55.4, 55.3, 53.5, 52.6, 49.2, 25.6; ESI-MS: *m/z* 478.2 $[M + H]^+$. HRMS (ESI) *m/z* calcd for $C_{27}H_{35}N_5O_3$ $[M + H]^+$ 478.2813, found: 478.2808.

*4-(4-(2,6-Dichlorobenzyl)piperazin-1-yl)-7-methoxy-6-[3-(4-morpholinyl)propoxy]quinazoline (**C2**).* Yield 7%, 0.05 g; yellow oily substance; ^{1}H NMR (CD_3OD, 500 MHz): δ

8.43 (s, 1H), 7.35 (d, $J=8.0$ Hz, 2H), 7.22 (t, $J=8.0$ Hz, 1H), 7.11 (s, 1H), 7.10 (s, 1H), 4.12 (t, $J=6.0$ Hz, 2H), 3.94 (s, 3H), 3.82 (s, 2H), 3.63–3.69 (m, 8H), 2.74 (t, $J=4.6$ Hz, 4H), 2.49–2.57 (m, 6H), 2.03–2.06 (br, m, 2H); ^{13}C NMR (CD_3OD, 125 MHz): δ 163.6, 155.5, 152.0, 148.2, 148.1, 136.8, 133.7, 129.4, 128.3, 110.9, 105.8, 104.6, 66.9, 66.3, 56.0, 55.4, 55.3, 53.5, 52.7, 49.4, 25.7; ESI-MS: *m/z* 546.4 $[M+H]^+$. HRMS (ESI) *m/z* calcd for $C_{27}H_{33}Cl_2N_5O_3$ $[M+H]^+$ 546.2033, found: 546.2026.

*4-(4-(2-Methylbenzyl)piperazin-1-yl)-7-methoxy-6-[3-(4-morpholinyl)propoxy]quinazoline (**C3**).* Yield 17%, 0.12 g; yellow oily substance; ^{1}H NMR (CD_3OD, 500 MHz): δ 8.38 (s, 1H), 6.91–7.13 (br, m, 6H), 3.99 (t, $J=6.0$ Hz, 2H), 3.86 (s, 3H), 3.61 (t, $J=4.6$ Hz, 4H), 3.41–3.51 (br, m, 4H), 3.39 (s, 2H), 2.46–2.49 (m, 6H), 2.27–2.39 (br, m, 7H), 1.94–1.97 (br, m, 2H); ^{13}C NMR (CD_3OD, 125 MHz): δ 163.5, 163.4, 155.2, 152.1, 147.9, 137.4, 135.6, 130.2, 129.9, 127.2, 125.4, 110.7, 106.0, 104.3, 67.0, 66.4, 60.5, 55.4, 55.3, 53.5, 52.8, 49.4, 25.7, 18.4; ESI-MS: *m/z* 492.5$[M+H]^+$. HRMS (ESI) *m/z* calcd for $C_{28}H_{37}N_5O_3$ $[M+H]^+$ 492.2969, found: 492.2963.

*4-(4-(3-Methylbenzyl)piperazin-1-yl)-7-methoxy-6-[3-(4-morpholinyl)propoxy]quinazoline (**C4**).* Yield 15 %, 0.11 g; yellow oily substance; ^{1}H NMR (CD_3OD, 500 MHz): δ 8.39 (s, 1H), 7.12 (t, $J=7.5$ Hz, 1H), 7.04–7.08 (m, 2H), 6.98–7.00 (m, 2H), 6.94 (s, 1H), 4.02 (t, $J=6.0$ Hz, 2H), 3.88 (s, 3H), 3.63 (t, $J=2.1$ Hz, 4H), 3.58 (s, 4H), 3.42 (s, 2H), 2.40–2.53 (m, 6H), 2.25–2.40 (br, m, 7H), 1.96–1.99 (br, m, 2H); ^{13}C NMR (CD_3OD, 125 MHz): δ 163.4, 155.2, 152.1, 148.1, 148.0, 137.7, 137.1, 129.9, 128.0, 127.9, 126.4, 110.8, 105.9, 104.3, 66.9, 66.4, 62.7, 55.4, 55.3, 53.5, 52.7, 49.2, 25.8, 20.4; ESI-MS: *m/z* 492.5 $[M+H]^+$. HRMS (ESI) *m/z* calcd for $C_{28}H_{37}N_5O_3$ $[M+H]^+$ 492.2969, found: 492.2966.

*4-(4-(4-Methylbenzyl)piperazin-1-yl)-7-methoxy-6-[3-(4-morpholinyl)propoxy]quinazoline (**C5**).* Yield 14%, 0.10 g; yellow oily substance; ^{1}H NMR (CD_3OD, 500 MHz): δ 8.59 (s, 1H), 8.42 (s, 1H), 7.85 (t, $J=9.9$ Hz, 2H), 7.45 (t, $J=8.2$ Hz, 2H), 7.06 (s, 2H), 4.10 (t, $J=5.7$ Hz, 2H), 3.93 (s, 3H), 3.74 (br, s, 6H), 3.65 (t, $J=4.6$ Hz, 4H), 3.29 (s, 3H), 2.80 (t, $J=4.6$ Hz, 4H), 2.54 (t, $J=7.3$ Hz, 2H), 2.46 (s, 3H), 2.01–2.04 (br, m, 2H); ^{13}C NMR (CD_3OD, 125 MHz): δ 163.6, 155.4, 152.0, 148.2, 148.0, 136.9, 133.9, 129.3, 128.7, 110.9, 105.9, 104.4, 66.9, 66.4, 62.4, 55.4, 55.3, 53.5, 52.6, 49.2, 25.7, 19.9; ESI-MS: *m/z* 492.5 $[M+H]^+$. HRMS (ESI) *m/z* calcd for $C_{28}H_{37}N_5O_3$ $[M+H]^+$ 492.2969, found: 492.2962.

*2-(4-(7-Methoxy-6-(3-morpholinopropoxy)quinazolin-4-yl)piperazin-1-yl)-*N*-phenylacetamide (**C6**).* Yield 13%, 0.10 g; yellow oily substance; ^{1}H NMR (CD_3OD, 500 MHz): δ 8.43 (s, 1H), 7.57 (d, $J=8.0$ Hz, 2H), 7.26 (d, $J=9.2$ Hz, 2H), 7.06 (s, 1H), 7.04 (s, 2H), 4.09 (t, $J=6.0$ Hz, 2H), 3.92 (s, 3H), 3.72 (s, 4H), 3.64 (t, $J=4.9$ Hz, 4H), 3.23 (s, 2H), 2.76 (t, $J=4.5$ Hz, 4H), 2.54 (t, $J=7.5$ Hz, 2H), 2.45 (s, 4H), 2.45–2.52 (m, 4H), 2.02–2.03 (br, m, 2H); ^{13}C NMR (CD_3OD, 125 MHz): δ 169.3, 163.5, 155.4, 152.0, 148.2, 148.0, 137.9, 128.6, 124.8, 120.0, 110.9, 105.9, 104.3, 67.0, 66.3, 61.6, 55.4, 55.3, 53.5, 52.9, 49.3, 25.7; ESI-MS: *m/z* 521.4 $[M+H]^+$. HRMS (ESI) *m/z* calcd for $C_{28}H_{36}N_6O_4$ $[M+H]^+$ 521.2871, found: 521.2863.

*2-(4-(7-Methoxy-6-(3-morpholinopropoxy)quinazolin-4-yl)piperazin-1-yl)-*N*-(o-methylphenyl)acetamide (**C7**).* Yield 13%, 0.10 g; yellow oily substance; ^{1}H NMR (CD_3OD, 500 MHz): δ 8.46 (s, 1H), 7.69 (d, $J=8.3$ Hz, 1H), 7.03–7.18 (m, 5H), 4.12 (t, $J=6.2$ Hz, 2H), 3.94 (s, 3H), 3.67–3.74 (m, 8H), 3.26 (s, 2H), 2.82 (t, $J=4.6$ Hz, 4H), 2.56 (t, $J=7.6$ Hz, 2H), 2.47 (s, 4H), 2.27 (s, 3H), 2.03–2.06 (br, m, 2H); ^{13}C NMR (CD_3OD, 125 MHz): δ 169.5, 163.6, 155.5, 152.0, 148.3, 148.1, 135.4, 130.2, 130.1, 126.3, 125.3, 123.0, 111.0, 105.9, 104.3, 67.3, 66.3, 61.4, 55.4, 55.3, 53.5, 53.0, 49.6, 25.7, 16.9; ESI-MS: *m/z* 535.5 $[M+H]^+$. HRMS (ESI) *m/z* calcd for $C_{29}H_{38}N_6O_4$ $[M+H]^+$ 535.3027, found: 535.3019.

*2-(4-(7-Methoxy-6-(3-morpholinopropoxy)quinazolin-4-yl)piperazin-1-yl)-*N*-(p-methylphenyl)acetamide (**C8**).* Yield 16%, 0.13 g; yellow oily substance; ^{1}H NMR (CD_3OD, 500 MHz): δ 8.74 (s, 1H), 7.44 (d, $J=8.6$ Hz, 2H), 7.16 (d, $J=11.5$ Hz, 2H), 7.11 (d, $J=8.6$ Hz, 2H), 4.16 (t, $J=6.0$ Hz, 2H), 3.96 (s, 3H), 3.80 (s, 4H), 3.69 (t, $J=4.6$ Hz, 4H), 3.25 (s, 2H), 2.80 (t, $J=4.6$ Hz, 4H), 2.61 (t, $J=7.5$ Hz, 2H), 2.53 (s, 4H), 2.28 (s, 3H), 2.05–2.08 (br, m, 2H); ^{13}C NMR (CD_3OD, 125 MHz): δ 169.3, 163.7, 155.6, 152.0, 148.3, 148.1, 135.2, 134.0, 128.9, 120.2, 110.9, 105.8, 104.5, 66.9, 66.2, 61.5, 55.4, 55.3, 53.4, 52.8, 49.3, 25.6, 19.6; ESI-MS: *m/z* 535.5 $[M+H]^+$. HRMS (ESI) *m/z* calcd for $C_{29}H_{38}N_6O_4$ $[M+H]^+$ 535.3027, found: 530.3018.

N*-(3-Chlorophenyl)-2-(4-(7-methoxy-6-(3-morpholinopropoxy)quinazolin-4-yl)piperazin-1-yl)acetamide (**C9**).* Yield 15%, 0.12 g; yellow oily substance; ^{1}H NMR (CD_3OD, 500 MHz): δ 8.41 (s, 1H), 7.74 (t, $J=2.5$ Hz, 1H), 7.40–7.42 (m, 2H), 7.17–7.21 (m, 1H), 6.97–7.03 (m, 2H), 4.06 (t, $J=6.0$ Hz, 2H), 3.91 (s, 3H), 3.63–3.69 (m, 8H), 3.21 (s, 2H), 2.74 (t, $J=7.4$ Hz, 4H), 2.43–2.51 (m, 6H), 1.99–2.02 (br, m, 2H); ^{13}C NMR (CD_3OD, 125 MHz): δ 169.5, 163.5, 155.3, 152.0, 148.1, 148.0, 139.4, 134.0, 129.8, 123.8, 119.7, 117.9, 110.9, 105.9, 104.3, 67.0, 66.3, 61.6, 55.4, 55.3, 53.4, 52.8, 49.3, 25.7; ESI-MS: *m/z* 555.4 $[M+H]^+$. HRMS (ESI) *m/z* calcd for $C_{28}H_{35}ClN_6O_4$ $[M+H]^+$ 555.2481, found: 555.2474.

*2-(4-(7-Methoxy-6-(3-morpholinopropoxy)quinazolin-4-yl)piperazin-1-yl)-*N*-(2-nitrophenyl)acetamide (**C10**).* Yield 8%, 0.07 g; yellow oily substance; ^{1}H NMR (CD_3OD, 500 MHz): δ 8.66 (d, $J=7.3$ Hz, 1H), 8.44 (s, 1H), 8.14 (d, $J=6.6$ Hz, 1H), 7.66 (t, $J=7.1$ Hz, 1H), 7.22 (t, $J=7.8$ Hz, 1H), 7.11 (d, $J=9.6$ Hz, 2H), 4.13 (t, $J=6.2$ Hz, 2H), 3.94 (s, 3H), 3.84 (m, 4H), 3.67 (t, $J=4.6$ Hz, 4H), 3.29 (s, 2H), 2.82 (t, $J=4.6$ Hz, 4H), 2.57 (t, $J=7.6$ Hz, 2H), 2.48 (s, 4H), 2.03–2.06 (br, m, 2H); ^{13}C NMR (CD_3OD, 125 MHz): δ 170.7, 163.6, 155.5, 152.0, 148.3, 148.1, 137.3, 135.3, 125.5, 123.7, 121.9, 110.9, 106.0, 104.6, 67.2, 66.3, 61.7, 61.5, 55.4, 53.4, 52.9, 49.5, 25.7; ESI-MS: *m/z* 566.4 $[M+H]^+$. HRMS (ESI) *m/z* calcd for $C_{28}H_{35}N_7O_6$ $[M+H]^+$ 566.2722, found: 566.2716.

Biological activity

The antitumor activities of the products against A549, K562, HepG2, and PC-3 were tested at five concentrations (0.625, 1.25, 2.5, 5, and 10 μM). Each test was done five times and assessed according to the MTT assay. The cell cultures were obtained from the Kunming Cell Bank. PC-3 was cultured at 37 °C and 5% CO_2 in Dulbecco's modified eagle medium supplemented with 10% fetal bovine serum and 1% penicillin streptomycin. A549, K562, and HepG2 cells were cultured in Roswell Park Memorial Institute (RPMI) 1640 supplemented with the same mixture. The cells were inoculated in a 96-well plate in 180 μL aliquots at 3×10^4 cells/mL and cultivated for 1 day. The plates were further incubated for 48 h, and the assay was terminated by the addition of 20 μL of 5 mg/mL MTT. Incubation with the dye was continued for 4 h, after which time the medium was removed and the dye was extracted from the cells with 150 μL of DMSO. The absorbance was measured with a Microplate Reader (TECAN infinite M200 pro, TECAN, Switzerland) at 490 nm wavelength. The growth percentage was calculated on a plate by plate basis for test wells relative to control wells. The sensitivity of the cancer cells to each test compound was expressed in terms of IC_{50}, indicated as mean values ± SD for three independent experiments. Statistical analysis was performed using GraphPad Prism (version 7) for the Student's test. Values of $p < .05$ were considered significant.

The wound healing assay was as follows. Cells were seeded in a six-well plate and grown for 24 h to 80% to 90% confluence. Cells were washed twice with phosphate-buffered saline (PBS), and the monolayers were scraped with a micropipette tip to create a uniform scratch. Next, cells were washed with PBS again to remove the detached cells. The compounds were added in the RPMI medium at 5 μM. DMSO was used as a control. Digital images of the wounded monolayers were obtained using a photomicroscope (Ti-S, Nikon, Japan) at 0, 6, 12, and 24 h. The unfilled scratched zones were quantified by Java's ImageJ software.[23,24]

Antiproliferative activity was measured by the clonogenic survival assay after treating with the test compound. Briefly, cells were seeded in a six-well plate at 3×10^5 cells/well and were stimulated by a range of compound doses (1.25, 2.5, 5, 10, and 20 μM). The plates were further incubated for 24 h and the cells were plated in six wells at 1000 cells per well cultured for 12 days, and the number of surviving colonies (defined as a colony with >50 cells) was counted. The survival fraction was calculated as the number of colonies divided by the number of cells seeded times plating efficiency. Three independent experiments were performed.[25,26]

Hoechst staining of the cultured cells was used to observe apoptotic nuclei by evaluation of nuclear morphology using a fluorescence inverted microscope. Cells were fixed in 4% paraformaldehyde solution for 10 min at RT. Then the cells were incubated with Hoechst 33258 dye for 20 min. Next, the cells were rinsed with precooling PBS and were observed under a fluorescence inverted microscope with 20 μL of antifluorescent quencher after air-drying. Typical nuclei showed non-condensed chromatin distributed over the whole nucleus. In contrast, apoptotic nuclei were identified by nuclear fragmentation of condensed chromatin.[27]

Flow cytometry

To evaluate cell apoptosis, a double staining trial with propidium iodide (PI) and fluorescein isothiocyanate isomer (FITC)-conjugated Annexin V (Solabio, Beijing, China) was performed. Cells were seeded in a six-well plate at 1×10^6 cells/well and were stimulated by a range of compound doses (5, 10, and 20 μM). The original culture medium was collected and the cells were cultured with trypsin, which were subsequently washed twice in binding buffer. Next, 5 μL of Annexin V-FITC and 5 μL of PI were adopted for dying cells for 15 min at RT. The apoptotic A549 and PC-3 cells were observed via flow cytometry (BD Accuri™ C6, BD Biosciences, USA) equipment.[28,29]

Declaration of conflicting interests

The author(s) declared no potential conflicts of interest with respect to the research, authorship, and/or publication of this article.

Funding

The author(s) disclosed receipt of the following financial support for the research, authorship, and/or publication of this article: This study was supported by the National Natural Science Foundation of China (No. 21867004); the Project of the State Key Laboratory of Functions and Applications of Medicinal Plants, Guizhou Medical University (No. FAMP2018); and the Science Technology Program of Guizhou Province (No. 20185781).

ORCID iD

Zhen-Chao Wang https://orcid.org/0000-0003-1859-0128

Supplemental material

Supplemental material for this article is available online.

References

1. Zhou Y, Murphy DE, Sun Z, et al. *Tetrahedron Lett* 2004; 45: 8049.
2. Habib NS, Ismail KA and Abdel-Aziem T. *Pharmazie* 2000; 55: 495.
3. Georgey HH, Abdel-Gawad N and Abbas S. *Molecules* 2008; 13: 2557.
4. Xue S, McKenna J and Shieh WC. *J Org Chem* 2004, 69: 6474.
5. Jessy EM, Sambanthan AT and Alex J. *Indian J Pharm Sci* 2007; 69: 476.
6. Wu X, Li M and Tang W. *Chem Biol Drug Des* 2011; 78: 932.
7. Thomas ES and Mark AS. *The Oncologist* 2008; 13: 933.
8. Sharma MJ, Kumar MS and Murahari M. *Arch Pharm* 2019; 352: 1800381.
9. Friedmann B, Caplin M and Hartley JA. *Clin Cancer Res* 2004; 10: 6476.
10. Wu X, Li M and Qu Y. *Bioorg Med Chem* 2010; 18: 3812.
11. Tomizawa Y, Fujita Y and Tamura A. *Lung Cancer* 2010; 68: 269.
12. Dominguez-Escrig JL, Kelly JD and Neal DE. *Clin Cancer Res* 2004; 10: 4874.

13. Zeng YD, Zhang L and Liao H. *Asian Pac J Cancer P* 2012; 13: 909.
14. Zheng Y, Li MD and Zhang SN. *J Chem Res* 2009; 2009: 388.
15. Yun CH, Boggon TJ and Li Y. *Cancer Cell* 2007; 11: 217.
16. Yang XB, Qin XL and Wang Q. *Heterocycl Commun* 2015; 21: 233.
17. Mao Z, Zheng X and Qi Y. *RSC Adv* 2016; 6: 7723.
18. Xu Y, Liang P and Ur Rashid H. *Med Chem Res* 2019; 28: 1618.
19. Yamamoto Y, Tanabe K and Okonogi T. *Chem Lett* 1999; 28: 103.
20. Solomon VR, Hu C and Lee H. *Bioorg Med Chem* 2010; 18: 1563.
21. Chen H, Zhang J and Hu P. *Bioorg Med Chem* 2019; 27: 115081.
22. Chandregowda V, Venkateshwara RG and Chandrasekhara RG. *Org Process Res Dev* 2007; 11: 813.
23. Chandregowda V, Rao VG and Reddy GC. *Heterocycles* 2007; 71: 39.
24. Hu S, Li L and Huang W. *Cancer Manag Res* 2018; 10: 4603.
25. Teixeira RR, Silva AMD and Siqueira RP. *J Brazil Chem Soc* 2019; 30: 541.
26. Feng XP, Yi H and Li MY. *Cancer Res* 2010; 70: 3450.
27. Li WQ, Yu HY and Zhong NZ. *In J Oncol* 2015; 46: 1601.
28. Kolomeichuk SN, Nizhnik YP and Makhova NN. *Chem Heterocycl Compd* 2018; 54: 70.
29. Lee CH, Lee KH and Jang AH. *Tuberculosis Respiratory Diseases* 2017; 80: 83.